ACS SyntheticBiology

Research Article

pubs.acs.org/synthbio

Genetic Manipulation of Outer Membrane Permeability: Generating Porous Heterogeneous Catalyst Analogs in *Escherichia coli*

Tushar N Patel,[†] Ah-Hyung Alissa Park,[‡] and Scott Banta*[,†]

[†]Department of Chemical Engineering, Columbia University, New York, New York 10027, United States

[‡]Department of Earth and Environmental Engineering, Columbia University, New York, New York 10027, United States

Supporting Information

ABSTRACT: The limited permeability of the *E. coli* outer membrane can significantly hinder whole-cell biocatalyst performance. In this study, the SARS coronavirus small envelope protein (SCVE) was expressed in *E. coli* cells previously engineered for periplasmic expression of carbonic anhydrase (CA) activity. This maneuver increased small molecule uptake by the cells, resulting in increased apparent CA activity of the biocatalysts. The enhancements in activity were quantified using methods developed for traditional heterogeneous catalysis. The expression of the SCVE protein was found to significantly reduce the Thiele moduli (ϕ), as well as increase the effectiveness factors (η), effective diffusivities (D_e), and permeabilities (P) of the biocatalysts. These catalytic improvements translated into superior performance of the biocatalysts for the precipitation of calcium carbonate from solution which is an attractive strategy for long-term sequestration of captured carbon dioxide. Overall, these results demonstrate that synthetic biology approaches can be used to enhance heterogeneous catalysts incorporated into microbial whole-cell scaffolds.

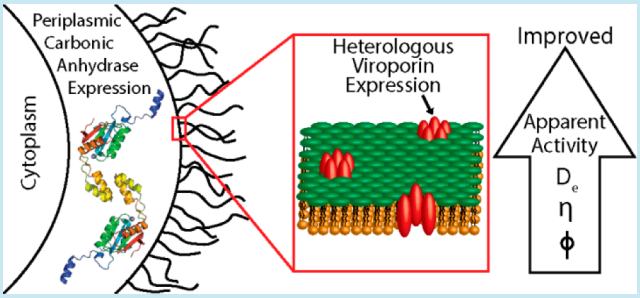

KEYWORDS: *biocatalysis, permeabilization, viroporin, cell diffusivity, thiele modulus, carbonic anhydrase*

As the field of synthetic biology matures, it is becoming clear that we are just beginning to understand the extent to which biological systems and parts can be designed, modified, and utilized to address critical needs. Recent examples include engineering of advanced batteries from biological templates,[1] enzymatic biomaterials,[2] biological logic gates,[3] and many other advances are clearly on the horizon.[4−6] Here, we explore the use of synthetic biology to create heterogeneous catalysts for the capture of carbon dioxide, which will be critical as we move toward the capture and utilization of carbon dioxide, or even the permanent sequestration of carbon dioxide from the atmosphere. To accomplish this goal, we have previously expressed CA enzymes in the periplasm of *E. coli*, and here, we explore whether improvements can be made in this system by reducing transport limitations via further genetic manipulation of the cells.

Gram-negative bacteria, such as *Escherichia coli*, have been previously shown to be less permeable than gram-positive bacteria, largely due to their outer membrane.[7] The native permeability through the outer membrane arises from porin proteins. The hydrophobic transmembrane α-helical domains of these proteins form tightly associated trimeric bundles that form nonspecific molecular transport channels.[8−13] Monomeric molecular weights of native porins can range from 28 to 48 kDa.[12] Common porins include OmpF, OmpC, and PhoE. Among all of the proteins within a cell, these are often the most prevalent on a mass basis. They typically form 10^5 channels per cell or more.[10] Transport through these channels is highly dependent on the properties of the solute, including physical size, charge, and hydrophobicity. In general, a typical porin generates a pore roughly 0.9−1.1 nm in diameter, and excludes molecules above 0.6 kDa.[8,13] In addition to porins, specific channels also exist in the outer membrane for the transport of maltose and maltodextrans (LamB), nucleotides (Tsx), and ferrichrome (FhuA), among others.[9]

Despite the presence of native porins, several chemical,[14−17] biological,[14,15,18−21] and genetic[14,22−25] treatments have been explored for outer membrane permeabilization. In most cases, these experiments were performed to better understand the structure and function of the outer membrane. More recent studies have examined the impact of permeabilization on biocatalysis,[26] as well as other whole-cell bioprocesses such as nutrient uptake.[27] One promising approach is the use of viroporins, which are a diverse class of viral proteins that further permeabilize the membranes of host cells.[28−30] Some viroporins encoded by bacteriophages are also referred to as holins.[31] Viroporins are similar to porins in that they oligomerize within the membrane to form pores, and this oligomerization often occurs between the hydrophobic, transmembrane, α-helical domains of the proteins.[29] Archetypal viroporins include the Picornavirus P2B, HCV p7, IAV M2, and

Received: December 6, 2013
Published: February 4, 2014

HIV-1 Vpu proteins.[30] Viroporins also possess similar exclusion sizes to porins, only allowing diffusion of small molecules.[32]

In this study, the SARS (severe acute respiratory syndrome) coronavirus envelope (SCVE) protein was evaluated for its ability to permeabilize the outer membrane of *E. coli*. The 76 amino acid SCVE protein is predominantly hydrophobic and each monomer contains one transmembrane domain, which when expressed on its own, can oligomerize into dimeric, trimeric, or pentameric bundles.[33] However, when the full protein is expressed, only homopentamers are observed *in vivo*.[34] These bundles were determined to be formed due to two cysteines at positions 40 and 44. Mutations at these sites rendered the protein inactive and unable to form transmembrane pores.[32] The pores formed by the SCVE protein are estimated to have a radius of about 0.6 nm[33] and preferentially facilitate transport of monovalent cations as opposed to monovalent anions.[35] Recently, SCVE was expressed in *E. coli* and was shown to improve the diffusion of two different small molecules across the outer membrane.[32] Therefore, recombinant expression of SCVE is a promising approach for modulating transport across the outer membrane of *E. coli*.

Whole-cell biocatalysts containing carbonic anhydrase (CA; EC 4.2.1.1) as their enzymatic component have recently emerged as a cost-effective method for catalyzing the hydration reaction of carbon dioxide (CO_2).[36−39] CAs are Zn^{2+}-binding metalloenzymes that are able to reversibly catalyze the hydration of aqueous CO_2 via the reaction mechanism below, where "EZn" represents the enzyme molecule and the bound Zn^{2+} ion:[40,41]

$$EZnH_2O \rightleftharpoons EZnOH^- + H^+ \quad (1)$$

$$EZnOH^- + CO_2 \rightleftharpoons EZnHCO_3^- \quad (2)$$

$$EZnHCO_3^- + H_2O \rightleftharpoons EZnH_2O + HCO_3^- \quad (3)$$

$$HCO_3^- \rightleftharpoons CO_3^{-2} + H^+ \quad (4)$$

Two isoforms of CA were selected for this study: carbonic anhydrase beta (Cab; *Methanobacterium thermoautotriphicum*; PDB 1G5C)[42] and carbonic anhydrase methanosarcina (Cam; *Methanosarcina thermophila*; PDB 1THJ).[43] We have previously reported the periplasmic expression of these isoforms in *E. coli*, resulting in functional whole cell biocatalysts; however, the activity was decreased as compared to the activity of the purified enzymes due to membrane transport limitations.[36]

Therefore, in this study the whole-cell biocatalysts were modified by SCVE expression and subsequently characterized. In addition to determining whether improvements in transport increase the overall apparent activity, the performance of the biocatalysts in accelerating carbonate precipitation was also explored to demonstrate functional utility. The ability to separately alter activity and transport in the whole cells via genetic engineering opens the door to better biocatalyst design, and thus, we explore the impact of the permeabilization on heterogeneous catalysis via estimation of the Thiele modulus and effectiveness factor for the system.

RESULTS AND DISCUSSION

Expression of SCVE. The SCVE gene was cloned into the pET-2Z vector, and this was transformed into BLR(DE3) cells, as well as cells containing CA-encoding plasmids using orthogonal antibiotics for selection. The presence of both plasmids in the cells was verified by PCR amplification of both genes. The three whole-cell biocatalysts were named BLR-SCVE, BLR-gCab/SCVE, and BLR-gCam/SCVE. Differential induction of the two different transgenes was accomplished with IPTG for SCVE and arabinose for CA.

Growth Inhibition Curves. To demonstrate the effect of SCVE expression on cell viability and growth rates, the OD at 600 nm of the induced and uninduced cultures were measured every hour for 4 h (Figure 1). As expected,[32] the induced

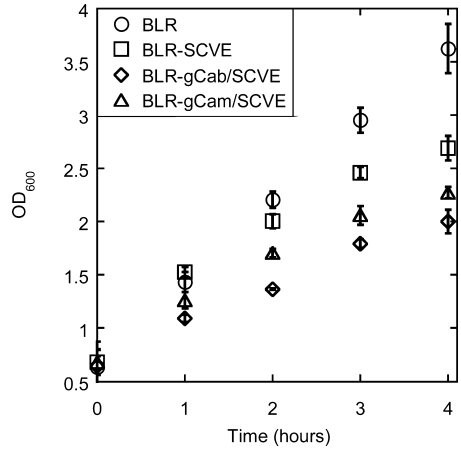

Figure 1. Growth retardation curves presented as OD_{600} vs time postinduction for all whole-cell biocatalysts evaluated. All measurements were performed in triplicate, with the error bars representing the standard deviations from the means.

cultures exhibited slower growth as compared to uninduced controls. After 4 h, the uninduced control cells reached a mean OD_{600} of 3.6. Conversely, BLR-SCVE, BLR-gCab/SCVE, and BLR-gCam/SCVE reached mean final OD_{600} values of 2.7, 2.0, and 2.3, respectively. The diminished growth is indicative of SCVE protein expression. However, the growth inhibition is not anticipated to be problematic during the utilization of the biocatalysts, as they will not be growing during the carbon capture process.

NPN Permeability. The NPN assay was used to quantify small molecule transport across the outer membrane. The uptake factors, calculated by dividing the background-corrected fluorescence value of each sample by the background corrected fluorescence of NPN alone,[44] of induced and uninduced cells harboring the pET2Z-SCVE plasmid can be seen in Figure 2. Native BLR cells harboring no recombinant plasmids yielded an uptake factor of 8.0 ± 0.3. BLR-SCVE, BLR-gCab/SCVE, and BLR-gCam/SCVE cells exhibited uptake factors of 9.4 ± 0.2, 9.1 ± 0.5, and 8.5 ± 0.2, respectively. ANOVA on this data indicated a statistically significant difference between the uptake factors of the control cells and each of the permeabilized cells. Posthoc analysis revealed no statistically significant difference between BLR-SCVE and BLR-gCab/SCVE cells. These results confirmed that small molecule transport across the outer membrane of *E. coli* cells was enhanced after expression of the SCVE protein.

Enhanced CA Activity. To determine the effect of the SCVE proteins on CA-activity of the whole-cell biocatalysts, apparent activity measurements were performed. The Michaelis−Menten kinetic parameters for native and altered whole-cell biocatalysts can be seen in Table 1. The apparent parameters for unpermeabilized BLR-gCab and BLR-gCam were previously published.[36] The rates of the cells expressing the SCVE protein

dx.doi.org/10.1021/sb400202s | ACS Synth. Biol. 2014, 3, 848−854

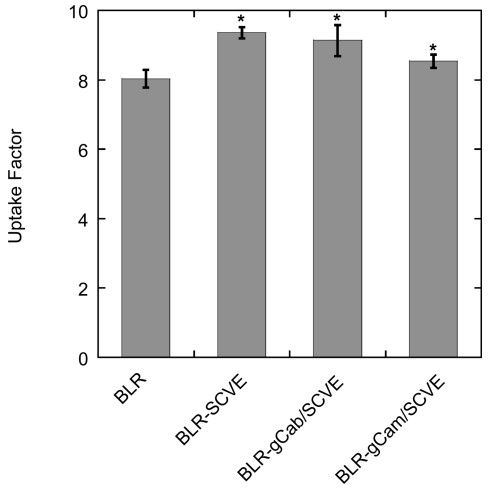

Figure 2. 1-N-phenylnaphthylamine (NPN) uptake factors for the various whole-cell biocatalysts evaluated. Uptake factors are defined as the fluorescence of the biocatalyst divided by the fluorescence of the NPN solution alone. All measurements were performed in triplicate, with the error bars representing the standard deviations from the means. * indicates statistically significant increase in uptake factor relative to controls.

Table 1. Kinetic Parameters for Unpermeabilized and Permeabilized Whole-Cell Biocatalysts

catalyst	V_{max}/cell (mM s^{-1} $cell^{-1}$)	K_M (mM)	$V_{max}/(K_M \cdot cell)$ (s^{-1} $cell^{-1}$)
BLR-gCab[a]	$2.5 \pm 0.6 \times 10^{-7}$	38 ± 5	6.5×10^{-9}
BLR-gCab/SCVE	$3.2 \pm 0.4 \times 10^{-7}$	38 ± 2	8.4×10^{-9}
BLR-gCam[a]	$1.9 \pm 0.4 \times 10^{-7}$	31 ± 3	6.0×10^{-9}
BLR-gCam/SCVE	$2.7 \pm 0.5 \times 10^{-7}$	34 ± 2	8.0×10^{-9}

[a]Previously published values.[36] Measurements were performed in triplicate, with errors indicating standard deviations from the means.

were corrected for the reaction rates of BLR-SCVE cells, which contain no recombinant CA. For the four whole-cell biocatalysts evaluated, almost no difference in the apparent K_M was seen (38 mM for BLR-gCab and BLR-gCab/SCVE; 31 mM for BLR-gCam and 34 mM for BLR-gCam/SCVE). Conversely, the per-cell rates of the cells expressing SCVE were higher (3.2×10^{-7} mM s^{-1} $cell^{-1}$ for BLR-gCab/SCVE and 2.7×10^{-7} mM s^{-1} $cell^{-1}$) than the unpermeabilized controls (2.5×10^{-7} mM s^{-1} $cell^{-1}$ for BLR-gCab and 1.9×10^{-7} mM s^{-1} $cell^{-1}$ for BLR-gCam). These results translate into 29% and 45% enhancements in apparent rate for BLR-gCab/SCVE and BLR-gCam/SCVE cells, respectively, as compared to BLR-gCab and BLR-gCam cells, respectively. Since Cam is the more active CA isoform, it is reasonable to expect cells harboring Cam to experience a larger degree of enhancement upon permeabilization as the kinetics become less impeded by transport limitations. Also, due to lower levels of protein loading in the BLR-gCam cells,[36] it is not surprising that the apparent kinetic values do not exceed those of BLR-gCab/SCVE. For both Cab and Cam, these results indicate an increase in diffusion rates of substrate and product across the outer membrane produces increases in the overall apparent reaction rates.

Increased Functional Activity. A model system for carbon mineralization was explored to demonstrate the functional utility of the biocatalysts. Carbon mineralization is a process by which CO_2 is converted to carbonate ions, which combine with divalent cations and precipitate as a thermodynamically stable salt.[39] The mineralization capabilities for the biocatalysts generated in this study were determined by converting gaseous CO_2 into calcium carbonate. The masses of $CaCO_3$ precipitated in the presence of various whole-cell biocatalysts can be seen in Figure 3. BLR and BLR-SCVE cells

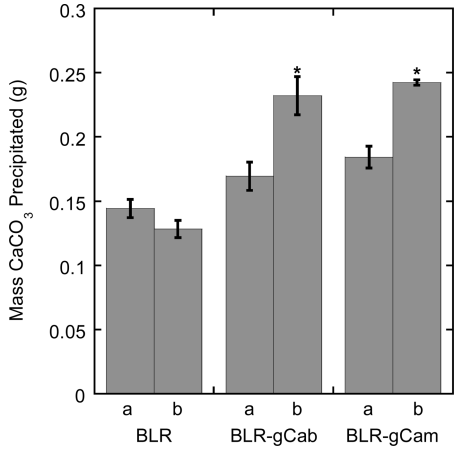

Figure 3. Calcium carbonate ($CaCO_3$) precipitation amounts for the various whole-cell biocatalysts evaluated. In each case, the cells were tested (a) without SCVE expression and (b) with SCVE expression. All measurements were performed in triplicate, with the error bars representing the standard deviations from the means. * indicates statistically significant improvement in precipitation relative to controls.

expressing no recombinant CA exhibited similar amounts of precipitation, with means of 0.14 and 0.13 g, respectively. The remaining whole-cells yielded mean masses of 0.17, 0.18, 0.23, and 0.24 g of $CaCO_3$ precipitated for BLR-gCab, BLR-gCam, BLR-gCab/SCVE, and BLR-gCam/SCVE, respectively. These values represent improvements in carbon mineralization of 35% and 33% for BLR-gCab and BLR-gCam, respectively, upon SCVE expression.

Two-way ANOVA on this data revealed that cells expressing recombinant CA exhibited statistically significantly higher levels of precipitation than those containing no CA. Also, whole-cell biocatalysts expressing the SCVE protein were found to be statistically significantly different from cells not expressing the protein. Posthoc analysis revealed no statistical significance in the difference between BLR-gCab/SCVE and BLR-gCam/SCVE, BLR-gCab and BLR-gCam, or BLR and BLR-SCVE cells. These results definitively show an improvement in CO_2 hydration and mineralization upon concomitant expression of CA and SCVE.

Diffusion/Reaction Quantification. The ability to modify both the activity and transport in the biocatalysts allows for the characterization of the system using classical methods developed in the heterogeneous catalysis literature. The effectiveness factor (η)[45] is defined as the whole-cell activity divided by the activity of an equivalent amount of enzyme with no transport barrier. In order to determine the equivalent amount of enzyme for a given number of whole-cell biocatalysts, previously published values for periplasmic loading were used.[36] The effectiveness factor can also be used to

dx.doi.org/10.1021/sb400202s | ACS Synth. Biol. 2014, 3, 848−854

calculate the Thiele modulus (ϕ), a dimensionless parameter that relates the diffusivity and reaction rate of a catalyst.[45]

The Thiele modulus is obtained by performing a dimensionless shell balance on the catalyst considering both diffusion and reaction within the shell. Assuming a spherical catalyst with Michaelis–Menten kinetics, the nondimensionalized differential equation resulting from this derivation is

$$\frac{d^2\psi}{d\lambda^2} + \frac{2}{\lambda}\frac{d\psi}{d\lambda} - \phi^2\frac{\psi}{1+\beta\psi} = 0 \tag{5}$$

where

$$\phi = R\sqrt{\frac{V_{max}}{D_e K_M}} \tag{6}$$

and

$$\beta = \frac{C_S}{K_M} \tag{7}$$

In eqs 5–7, ψ is the nondimensionalized concentration (C/C_S), λ is the nondimensionalized radius (r/R), R is the radius of the catalyst, D_e is the effective diffusivity of the catalyst, and C_S is the bulk concentration of reactant (CO_2) in the extracellular space. Equation 5 can be solved numerically to determine the nondimensionalized concentration profile in the periplasm for each biocatalyst. For a full derivation of these expressions and the concentration profiles for each whole-cell biocatalyst evaluated, please refer to the Supporting Information. To obtain a value for ϕ, the following relationship between the effectiveness factor and Thiele modulus was used:[46]

$$\eta = \left(\frac{3\sqrt{2}}{\phi}\right)\frac{1+\beta}{\beta}\sqrt{\beta - \ln(1+\beta)} \tag{8}$$

Once the Thiele modulus was calculated, eq 6 was solved for D_e, which was then calculated.

The last parameter calculated to describe the whole-cell biocatalysts was the permeability (P) of the outer membrane to CO_2. The theoretical permeability of BLR-gCab and BLR-gCam was calculated by[47]

$$P = \left(\frac{D}{d}\right)\left(\frac{a_0}{A}\right)\left(\frac{a}{a_0}\right) \tag{9}$$

where D is the free diffusivity of CO_2 (1.94×10^3 $\mu m^2/s$),[48] d is the membrane thickness (7.8×10^{-3} μm),[49] a_0 is the cross-sectional area of all of the pores present in the outer membrane (0.113 μm^2),[47] A is the total surface area of the outer membrane (3.00 μm^2),[47] and a/a_0 is the Renkin correction factor, a relationship between the effective pore area (a) and a_0. It was calculated using[47]

$$\frac{a}{a_0} = \left[1 - \left(\frac{r_{CO2}}{R_p}\right)^2\right]\left[1 - 2.104\left(\frac{r_{CO2}}{R_p}\right) + 2.09\left(\frac{r_{CO2}}{R_p}\right)^3 - 0.95\left(\frac{r_{CO2}}{R_p}\right)^5\right] \tag{10}$$

where r_{CO2} is the solute radius and R_p is the pore radius (5.8 Å).[47] The solute radius of CO_2 was calculated by[50]

$$r_{CO2} = \sqrt[3]{\frac{3M}{4\pi\rho N_A}} \tag{11}$$

where M is the molecular weight of the solute (44 g/mol), ρ is the density of a solution of the solute being evaluated ($\rho_{CO2} = \rho_{H2O}$ = 1 g/mL), and N_A is Avogadro's number. Once P was calculated for BLR-gCab and BLR-gCam, it was used to calculate P for the cells expressing the SCVE protein. To do so, the following expression was used to determine a partition coefficient (K) as a function of D_e for both biocatalysts:[51]

$$P = \frac{KD_e}{d} \tag{12}$$

Then, using the D_e for each SCVE-expressing biocatalyst and its corresponding K, the permeability for the permeabilized cells was calculated. Table 2 contains the values for η, ϕ, D_e, and P for the four whole-cell biocatalysts quantified using these calculations.

Table 2. Parameters Describing Reaction-Diffusion Relationship for Whole-Cell Biocatalysts with and without SCVE Expression

catalyst	η	ϕ	D_e (μm^2 s^{-1})	P_{CO2} (μm s^{-1})
BLR-gCab	0.21	22	0.83×10^{-3}	1.7×10^3
BLR-gCab/SCVE	0.43	11	2.9×10^{-3}	4.1×10^3
BLR-gCam	0.28	17	2.0×10^{-3}	1.7×10^3
BLR-gCam/SCVE	0.58	8.1	7.3×10^{-3}	4.4×10^3

The calculations show an increase in effectiveness factor of about 100% upon permeabilization with SCVE expression for biocatalysts containing both Cab and Cam. This roughly translates into a 50% reduction in the Thiele modulus, a 3.5-fold increase in diffusivity, and an increase in permeability of about 2.5-fold. The biocatalyst found to have the highest permeability was BLR-gCam/SCVE, for which P was found to be approximately 4.4×10^3 $\mu m/s$. The calculated permeability was used to estimate the expression yield necessary to obtain such a value. By using the properties of an SCVE-generated pore described above, it was estimated that the expression yield would be 18 mg of SCVE per liter of culture in order to achieve this permeability. Previously published reports have shown recombinant porin expression yields of 20–25 mg/L of culture in *E. coli*.[52,53] Another report of outer-membrane protein expression showed a yield of 12 mg/L of culture after purification.[54] Given that the protein recovery from each step required in protein purification could be as low as 70%,[55] the actual yield could be much higher. Finally, the expression of native outer membrane proteins such as OmpA, OmpX, and OmpT have been shown to reach yields of 150–170 mg/L of culture in *E. coli*.[56] Thus, the estimated protein yield seems reasonable and consistent with values found by other groups.

CONCLUSIONS

Recombinant expression of the SCVE viroporins in *E. coli* resulted in the improvement of CA-based whole-cell biocatalysts. By introducing additional pores to the outer membrane of the cells, the diffusivity of small molecules across the outer membrane was enhanced. This translated into increased apparent catalytic activity. These improvements were measured experimentally, the data from which was then used to quantify the enhancement using principles of diffusion-reaction systems. This system could very easily be applied to

dx.doi.org/10.1021/sb400202s | ACS Synth. Biol. 2014, 3, 848–854

other biocatalysts whose catalytic components (most commonly enzymes) are relegated to the periplasmic space of the cell. Overall, this work demonstrates that synthetic biology techniques can be used to design and build improved heterogeneous catalysts, which will facilitate applications such as carbon capture and sequestration.

METHODS

Materials. Chemicals were obtained from Sigma-Aldrich (St. Louis, MO), unless otherwise stated. Custom oligonucelotides were synthesized by Integrated DNA Technologies (IDT; Coralville, IA). Enzymes used in cloning were purchased from New England Biolabs (NEB; Ipswich, MA). Isopropyl β-D-1-thiogalactopyranoside (IPTG) was obtained from Promega Corp. (Madison, WI). BLR(DE3) *E. coli* cells were from Novagen (Billerica, MA)

Cloning. The SCVE gene was synthesized by Epoch Life Science (Sugarland, TX). Oligonucleotides TP55 and TP56 were used to amplify the gene. The PCR product was then digested using the *Bam*HI and *Eco*RI restriction enzymes. The destination vector pET-2Z (Plasmid 29776; Addgene, Cambridge, MA) was similarly digested and gel-extracted. The digested SCVE fragments were ligated into the digested pET-2Z vector using T4 DNA Ligase, resulting in the plasmid pET2Z-SCVE. BLR(DE3) *E. coli* cells were transformed with this plasmid by electroporation and selected on agar plates containing 50 μg/mL spectinomycin. The pET2Z-SCVE plasmid was also transformed into BLR-gCab or BLR-gCam cells and selected on agar plates containing 50 μg/mL spectinomycin and 50 μg/mL ampicillin. These whole-cell biocatalysts were selected to allow for individual induction of CA and SCVE expression. The SCVE DNA and amino acid sequences, as well as the two primer sequences used for cloning can be found in Supporting Information Tables S1 and S2.

Protein Expression. SCVE was expressed at 37 °C in 10 mL of Luria Broth (LB) supplemented with 50 μg/mL spectinomycin. Cells containing gCab or gCam as well as SCVE were expressed in similar conditions but also contained 50 μg/mL ampicillin. Cultures were inoculated by diluting overnight cultures at a 1:50 ratio. SCVE expression was induced with 1 mM IPTG at OD_{600} = 0.6. Induction of gCab and gCam was performed by concurrently adding 0.02% L-arabinose and 1 mM $ZnCl_2$. After 4 h of expression, the cultures were pelleted by centrifugation at 3000*g* for 10 min. The pellets were resuspended in the buffer appropriate for the various assays described below.

NPN Assay. Several versions of a 1-N-phenylnaphthylamine (NPN) uptake assay have been described previously.[44,57,58] The basic principle is substrate fluorescence upon interaction with the inner lipid membrane and an increase in diffusivity would result in an increase in fluorescence. Here, the whole-cell biocatalysts were resuspended in 5 mM HEPES pH 7.2. A stock solution of NPN containing 5 mM NPN in acetone was diluted to 50 μM in 5 mM HEPES pH 7.2. In a black 96-well plate, 50 μL of 5 mM HEPES pH 7.2 and 100 μL of the cell suspensions were mixed. To initiate the reaction, 50 μL of the diluted NPN solution was added to the wells. After incubation at 25 °C for 3 min, the fluorescence was measured using excitation and emission wavelengths of 355 and 405 nm, respectively, in a SpectraMax M2 spectrophotometer (Sunnyvale, CA).

Kinetic Assays. The stopped-flow kinetic assay used was previously described.[36] Briefly, solutions of 55.6 μM *m*-cresol purple were saturated with CO_2 and N_2 via bubbling of each compressed gas through a glass gas dispersion tube (Ace Glass, Vineland, NJ) at 25 °C. These solutions were mixed to vary the concentration of CO_2 from 3 to 28 mM. The whole-cell biocatalysts were diluted in 100 mM Tris at pH 9.0. The concentration of cells in each solution was determined by measuring their optical densities at 600 nm. Using a BioLogic stopped-flow apparatus (BioLogic, Claix, Isère, France) attached to a Jasco J-815 CD Spectrometer (JASCO, Easton, MD), the absorbance at 578 nm was monitored. The data was fit to the differential form of the Michaelis−Menten equation using the Berkeley Madonna software.[59] Each measurement was baseline-corrected by the activity of BLR cells expressing no recombinant CA.

$CaCO_3$ Precipitation. The precipitation assay used was previously described.[36] Briefly, 5 mL of 1 M Tris pH 9.0 was placed in a 15 mL centrifuge tube (Corning, Inc., Tewksbury, MA). After adding the biocatalyst being tested, compressed CO_2 gas was bubbled through each solution for 30 s using a glass gas dispersion tube. Immediately after bubbling, calcium chloride ($CaCl_2$) and calcium carbonate ($CaCO_3$) were added to the solution. After incubation at 25 °C for 1 h, the suspension was passed through a spin column (Epoch Life Science, Sugarland, TX) on a vacuum manifold (Qiagen, Valencia, CA). Once they dried, the columns were weighed to determine their total mass. The amount of $CaCO_3$ generated in each sample was determined by subtracting the initial mass of the spin column, the mass of cells added, and the mass of $CaCO_3$ added.

Statistical Analysis. Analysis of variance (ANOVA) was performed using the Minitab program (Minitab Inc., State College, PA). The general linear model (GLM) and the Tukey Method were both used to evaluate the data.

ASSOCIATED CONTENT

Supporting Information

Sequence data and the derivation and solution of eq 5. This material is available free of charge via the Internet at http://pubs.acs.org.

AUTHOR INFORMATION

Corresponding Author

*Tel: 212-854-7531. Fax: 212-854-3054. E-mail: sbanta@columbia.edu.

Notes

The authors declare no competing financial interest.

ACKNOWLEDGMENTS

Funding for this work was provided by the U.S. Department of Energy (ARPA-E DE-AR0000100).

REFERENCES

(1) Nam, K. T., Kim, D. W., Yoo, P. J., Chiang, C. Y., Meethong, N., Hammond, P. T., Chiang, Y. M., and Belcher, A. M. (2006) Virus-enabled synthesis and assembly of nanowires for lithium ion battery electrodes. *Science 312*, 885−888.

(2) Kim, Y. H., Campbell, E., Yu, J., Minteer, S. D., and Banta, S. (2013) Complete oxidation of methanol in biobattery devices using a hydrogel created from three modified dehydrogenases. *Angew. Chem., Int. Ed. Engl. 52*, 1437−1440.

(3) Bonnet, J., Yin, P., Ortiz, M. E., Subsoontorn, P., and Endy, D. (2013) Amplifying genetic logic gates. *Science 340*, 599−603.

(4) Benner, S. A., and Sismour, A. M. (2005) Synthetic biology. *Nat. Rev. Genet. 6*, 533−543.

(5) Purnick, P. E., and Weiss, R. (2009) The second wave of synthetic biology: from modules to systems. *Nat. Rev. 10*, 410−422.
(6) Agapakis, C. M. (2013) Designing synthetic biology. *ACS Synth. Biol.*, DOI: 10.1021/sb4001068.
(7) Leive, L. (1974) The barrier function of the Gram-negative envelope. *Ann. N.Y. Acad. Sci. 235*, 109−129.
(8) Nikaido, H. (1993) Transport across the bacterial outer membrane. *J. Bioenergetics Biomembr. 25*, 581−589.
(9) Nikaido, H., and Vaara, M. (1985) Molecular basis of bacterial outer membrane permeability. *Microbiol. Rev. 49*, 1.
(10) Nikaido, H., and Rosenberg, E. Y. (1983) Porin channels in *Escherichia coli*: Studies with liposomes reconstituted from purified proteins. *J. Bacteriol. 153*, 241−252.
(11) Hancock, R. E., and Bell, A. (1988) Antibiotic uptake into gram-negative bacteria. *Eur. J. Clin. Microbiol. Infect. Dis. 7*, 713−720.
(12) Hancock, R. (1987) Role of porins in outer membrane permeability. *J. Bacteriol. 169*, 929.
(13) Benz, R., Janko, K., Boos, W., and Läuger, P. (1978) Formation of large, ion-permeable membrane channels by the matrix protein (porin) of *Escherichia coli* . *Biochim. Biophys. Acta 511*, 305−319.
(14) Hancock, R. E. (1984) Alterations in outer membrane permeability. *Annu. Rev. Microbiol. 38*, 237−264.
(15) Vaara, M. (1992) Agents that increase the permeability of the outer membrane. *Microbiol. Rev. 56*, 395−411.
(16) Irvin, R., MacAlister, T., and Costerton, J. (1981) Tris-(hydroxymethyl) aminomethane buffer modification of *Escherichia coli* outer membrane permeability. *J. Bacteriol. 145*, 1397−1403.
(17) Helander, I., Nurmiaho-Lassila, E.-L., Ahvenainen, R., Rhoades, J., and Roller, S. (2001) Chitosan disrupts the barrier properties of the outer membrane of Gram-negative bacteria. *Int. J. Food Microbiol. 71*, 235−244.
(18) Sotirova, A., Spasova, D., Galabova, D., Karpenko, E., and Shulga, A. (2008) Rhamnolipid−biosurfactant permeabilizing effects on gram-positive and gram-negative bacterial strains. *Curr. Microbiol. 56*, 639−644.
(19) Skerlavaj, B., Romeo, D., and Gennaro, R. (1990) Rapid membrane permeabilization and inhibition of vital functions of gram-negative bacteria by bactenecins. *Infect. Immun. 58*, 3724−3730.
(20) Johansen, C., Verheul, A., Gram, L., Gill, T., and Abee, T. (1997) Protamine-induced permeabilization of cell envelopes of gram-positive and gram-negative bacteria. *Appl. Environ. Microbiol. 63*, 1155−1159.
(21) Ibrahim, H. R., Thomas, U., and Pellegrini, A. (2001) A helix-loop-helix peptide at the upper lip of the active site cleft of lysozyme confers potent antimicrobial activity with membrane permeabilization action. *J. Biol. Chem. 276*, 43767−43774.
(22) Sampson, B. A., Misra, R., and Benson, S. A. (1989) Identification and characterization of a new gene of *Escherichia coli* K-12 involved in outer membrane permeability. *Genetics 122*, 491−501.
(23) Perez, M., García-Barreno, B., Melero, J. A., Carrasco, L., and Guinea, R. (1997) Membrane permeability changes induced in *Escherichia coli* by the SH protein of human respiratory syncytial virus. *Virology 235*, 342−351.
(24) Ma, D., Cook, D. N., Alberti, M., Pon, N. G., Nikaido, H., and Hearst, J. E. (1995) Genes acrA and acrB encode a stress-induced efflux system of *Escherichia coli*. *Mol. Microbiol. 16*, 45−55.
(25) Birkeland, N.-K. (1994) Cloning, molecular characterization, and expression of the genes encoding the lytic functions of lactococcal bacteriophage ϕLCE: A dual lysis system of modular design. *Can. J. Microbiol. 40*, 658−665.
(26) Ni, Y., and Chen, R. R. (2004) Accelerating whole-cell biocatalysis by reducing outer membrane permeability barrier. *Biotechnol. Bioeng. 87*, 804−811.
(27) Chen, R. R. (2007) Permeability issues in whole-cell bioprocesses and cellular membrane engineering. *Appl. Microbiol. Biotechnol. 74*, 730−738.
(28) Carrasco, L. (1995) Modification of membrane permeability by animal viruses. *Adv. Virus Res. 45*, 61−112.
(29) Gonzalez, M. E., and Carrasco, L. (2003) Viroporins. *FEBS Lett. 552*, 28−34.
(30) Nieva, J. L., Madan, V., and Carrasco, L. (2012) Viroporins: Structure and biological functions. *Nat. Rev. Microbiol. 10*, 563−574.
(31) Wang, I.-N., Smith, D. L., and Young, R. (2000) Holins: The protein clocks of bacteriophage infections. *Annu. Rev. Microbiol. 54*, 799−825.
(32) Liao, Y., Lescar, J., Tam, J., and Liu, D. (2004) Expression of SARS-coronavirus envelope protein in *Escherichia coli* cells alters membrane permeability. *Biochem. Biophys. Res. Commun. 325*, 374−380.
(33) Torres, J., Parthasarathy, K., Lin, X., Saravanan, R., Kukol, A., and Liu, D. X. (2006) Model of a putative pore: The pentameric α-helical bundle of SARS coronavirus E protein in lipid bilayers. *Biophys. J. 91*, 938−947.
(34) Parthasarathy, K., Ng, L., Lin, X., Liu, D. X., Pervushin, K., Gong, X., and Torres, J. (2008) Structural flexibility of the pentameric SARS coronavirus envelope protein ion channel. *Biophys. J. 95*, L39−L41.
(35) Wilson, L., Mckinlay, C., Gage, P., and Ewart, G. (2004) SARS coronavirus E protein forms cation-selective ion channels. *Virology 330*, 322−331.
(36) Patel, T. N., Park, A.-H. A., and Banta, S. (2013) Periplasmic expression of carbonic anhydrase in *Escherichia coli*: A new biocatalyst for CO_2 hydration. *Biotechnol. Bioeng. 110*, 1865−1873.
(37) Jo, B. H., Seo, J. H., Kang, D. G., and Cha, H. J. (2013) Engineered *Escherichia coli* with periplasmic carbonic anhydrase as a biocatalyst for CO_2 sequestration. *Appl. Environ. Microbiol. 79*, 6697−6705.
(38) Fan, L. H., Liu, N., Yu, M. R., Yang, S. T., and Chen, H. L. (2011) Cell surface display of carbonic anhydrase on *Escherichia coli* using ice nucleation protein for CO_2 sequestration. *Biotechnol. Bioeng. 108*, 2853−2864.
(39) Barbero, R., Carnelli, L., Simon, A., Kao, A., Monforte, A. d. A., Riccò, M., Bianchi, D., and Belcher, A. (2013) Engineered yeast for enhanced CO_2 mineralization. *Energy Environ. Sci. 6*, 660−674.
(40) Silverman, D. N., and Lindskog, S. (1988) The catalytic mechanism of carbonic anhydrase: Implications of a rate-limiting protolysis of water. *Acc. Chem. Res. 21*, 30−36.
(41) Lindskog, S. (1997) Structure and mechanism of carbonic anhydrase. *Pharmacol. Ther. 74*, 1.
(42) Smith, K. S., and Ferry, J. G. (1999) A plant-type (β-class) carbonic anhydrase in the thermophilic methanoarchaeon *Methanobacterium thermoautotrophicum*. *J. Bacteriol. 181*, 6247−6253.
(43) Alber, B. E., and Ferry, J. G. (1994) A carbonic anhydrase from the archaeon *Methanosarcina thermophila*. *Proc. Nat. Acad. Sci. 91*, 6909−6913.
(44) Helander, I., and Mattila-Sandholm, T. (2000) Fluorometric assessment of Gram-negative bacterial permeabilization. *J. Appl. Microbiol. 88*, 213−219.
(45) Fogler, H. S. (2006) *Elements of Chemical Reaction Engineering*, 4 ed., Prentice Hall, Englewood, NJ.
(46) Dutta, R. (2008) *Fundamentals of Biochemical Engineering*, Ane Books India, India.
(47) Nikaido, H., and Rosenberg, E. Y. (1981) Effect on solute size on diffusion rates through the transmembrane pores of the outer membrane of *Escherichia coli*. *J. Gen. Physiol. 77*, 121−135.
(48) Tamimi, A., Rinker, E. B., and Sandall, O. C. (1994) Diffusion coefficients for hydrogen sulfide, carbon dioxide, and nitrous oxide in water over the temperature range 293−368 K. *J. Chem. Eng. Data 39*, 330−332.
(49) Hobot, J., Carlemalm, E., Villiger, W., and Kellenberger, E. (1984) Periplasmic gel: New concept resulting from the reinvestigation of bacterial cell envelope ultrastructure by new methods. *J. Bacteriol. 160*, 143−152.
(50) Schultz, S. G., and Solomon, A. (1961) Determination of the effective hydrodynamic radii of small molecules by viscometry. *J. Gen. Physiol. 44*, 1189−1199.

(51) Zwolinski, B. J., Eyring, H., and Reese, C. E. (1949) Diffusion and membrane permeability. *J. Phys. Chem. 53*, 1426−1453.
(52) Schmid, B., Krömer, M., and Schulz, G. E. (1996) Expression of porin from *Rhodopseudomonas blastica* in *Escherichia coli* inclusion bodies and folding into exact native structure. *FEBS Lett. 381*, 111−114.
(53) Schmid, B., Maveyraud, L., Krömer, M., and Schulz, G. E. (1998) Porin mutants with new channel properties. *Protein Sci. 7*, 1603−1611.
(54) Mohanty, A. K., and Wiener, M. C. (2004) Membrane protein expression and production: Effects of polyhistidine tag length and position. *Protein Expression Purif. 33*, 311−325.
(55) Ward, W. W., and Swiatek, G. (2009) Protein purification. *Current Analytical Chemistry 5*, 85−105.
(56) Bannwarth, M., and Schulz, G. E. (2003) The expression of outer membrane proteins for crystallization. *Biochim. Biophys. Acta 1610*, 37−45.
(57) Alakomi, H.-L., Skyttä, E., Saarela, M., Mattila-Sandholm, T., Latva-Kala, K., and Helander, I. (2000) Lactic acid permeabilizes gram-negative bacteria by disrupting the outer membrane. *Appl. Environ. Microbiol. 66*, 2001−2005.
(58) Nieva-Gomez, D., and Gennis, R. B. (1977) Affinity of intact *Escherichia coli* for hydrophobic membrane probes is a function of the physiological state of the cells. *Proc. Nat. Acad. Sci. 74*, 1811−1815.
(59) Zahnley, T., Macey, R., and Oster, G. (2006) Berkeley Madonna, version 8.3.14, University of California, Berkeley, CA.